Veterinary Microbiology 233 (2019) 93–101

Contents lists available at ScienceDirect

Veterinary Microbiology

journal homepage: www.elsevier.com/locate/vetmic

Porcine circovirus type 2 promotes *Actinobacillus pleuropneumoniae* survival during coinfection of porcine alveolar macrophages by inhibiting ROS production

Wenxi Qi[a], Rining Zhu[a], Chuntong Bao[a], Jiameng Xiao[a], Baijun Liu[a], Ming Sun[a], Xin Feng[a], Jingmin Gu[a], Yang Li[a,*], Liancheng Lei[a,b,*]

[a] Key Laboratory of Zoonosis, Ministry of Education, Institute of Zoonosis/College of Veterinary Medicine, Jilin University, Changchun, Jilin, 130062, PR China
[b] College of Animal Science, Yangtze University, Jingzhou, Hubei, 434023, PR China

ARTICLE INFO

Keywords:
Actinobacillus pleuropneumoniae
Coinfection
Porcine circovirus type 2
Reactive oxygen species
Porcine alveolar macrophage

ABSTRACT

Actinobacillus pleuropneumoniae (APP) and *porcine circovirus* type 2 (PCV2) are both important pathogens of the porcine respiratory disease complex (PRDC), which results in significant worldwide economic losses. Recently, PCV2 and APP coinfection has been described in the worldwide pork industry, and represents an extremely complex situation in veterinary medicine. However, the mechanism of their coinfection has not been investigated. In this study, we found that PCV2 promoted APP adhesion to and invasion of porcine alveolar macrophages (PAMs) during coinfection. Additionally, PCV2 suppressed reactive oxygen species (ROS) production by inhibiting cytomembrane NADPH oxidase activity, which was beneficial for APP survival in PAMs in vitro. During coinfection, PCV2 weakened the inflammatory response and macrophage antigen presentation by decreasing TNF-α, IFN-γ and IL-4 expression, and reduced clearance of the invading bacteria. The host-cell experimental results were verified in a mouse model. The findings provide a deeper and novel understanding of porcine coinfection, and will be extremely helpful for the design of strategies for PRDC control.

1. Introduction

The porcine respiratory disease complex (PRDC) is a major obstacle responsible for substantial losses in the worldwide swine industry. The most important feature of PRDC is mixed infection by multiple pathogens such as *porcine reproductive and respiratory syndrome virus* (PRRSV), *porcine circovirus* type 2 (PCV2), *swine influenza virus* (SIV), *Actinobacillus pleuropneumoniae* (APP), and *Mycoplasma hyopneumoniae* (MHYO) (Opriessnig et al., 2011). The interactions between different pathogens play an important role in the development of and recovery from PRDC. Coinfection of SIV and APP has been reported to exacerbate lung lesions and accelerate SIV replication (Pomorska-Mól et al., 2017). Similarly, PRRSV and *Streptococus suis* coinfections of pigs enhances the virulence of the virus and increases susceptibility to the bacterium (Thanawongnuwech et al., 2000). Lipopolysaccharide from Gram-negative bacteria can increase PCV2 proliferation in porcine alveolar macrophages (PAMs) (Chang et al., 2006b).

APP is a Gram-negative, short, rod-shaped bacterium that is the causative agent of contagious porcine pleuropneumonia (Chiers et al., 2010). The clinical symptoms caused by APP include high fever, cough, and runny nose (Bossé et al., 2002). PCV2 is a single-stranded, circular, DNA virus (Ge et al., 2012). Piglets infected with PCV2 display clinical signs, including weight loss, enlarged lymph nodes, and jaundice. PCV2 depletes lymphocytes to cause immunosuppression in swine (Meng, 2013). APP and PCV2 coinfection is a frequent occurrence in PRDC (Cheong et al., 2017; Haimi-Hakala et al., 2017), and such combinations can affect productivity in pig production systems. (Dione et al., 2018).

PAMs are the first line of defense against invasion by pathogenic microorganisms into the lung and are located on the surface of the alveolar cavity (Allard et al., 2018; Joshi et al., 2018). PAMs participate in multiple biological processes, including immune surveillance, pathogen clearance, inflammatory responses, tissue repair, and maintenance of lung homeostasis (Murray and Wynn, 2011; Byrne et al., 2015). One defense mechanism of macrophages is the respiratory burst, the production of reactive oxygen species (ROS). ROS can directly kill pathogens (McCallum and Garsin, 2016). The majority of ROS are produced by mitochondria or nicotinamide adenine dinucleotide

* Corresponding authors at: Key Laboratory of Zoonosis, Ministry of Education, Institute of Zoonosis/College of Veterinary Medicine, Jilin University, Xi'an Road 5333, Changchun, China.
E-mail addresses: liyang_0317@jlu.edu.cn (Y. Li), leiliancheng@163.com (L. Lei).

https://doi.org/10.1016/j.vetmic.2019.04.028
Received 10 January 2019; Received in revised form 18 April 2019; Accepted 24 April 2019

phosphate (NADPH) oxidase (Vlahos and Selemidis, 2014; Scialò et al., 2017). Mitochondrial reactive oxygen species (mROS) are produced by electron transport chains (ETCs), with electrons leaking from ETCs reacting with oxygen to form superoxide radicals which can attack and kill pathogens (Banoth and Cassel, 2018). NADPH oxidase on the cell membrane is activated during the pathogen invasion process. Reduced coenzyme II (NADPH) is converted into oxidized coenzyme II (NADP), and the oxygen molecule gains a superoxide anion (O^{2-}) and subsequent reactions generate H_2O_2 and OH-. Superoxide anion production has the function of killing microorganisms (Lam et al., 2012).

Infection with either APP or PCV2 can cause serious damage in PAMs. APP has the ability to induce PAM apoptosis (Wang et al., 2015), while PCV2 infection results in decreased PAM microbicidal activity and disruption of cytokine expression (Chang et al., 2006a). However, the mechanism of PCV2 and APP coinfection is not understood. In this study, we investigated APP adhesion to, invasion of and survival in PAMs during coinfection with PCV2. ROS concentation, mitochondrial membrane potential, and cytomembrane NADPH oxidase activity were measured during infection in vitro. Simultaneously, changes in proinflammatory cytokines were detected during singular PCV2 or APP infection, and coinfection. Finally, the host-cellular experimental results were verified in vivo.

2. Materials and methods

2.1. Culture conditions

Immortalized PAMs (PAM-Tang) were donated by the Harbin Veterinary Research Institute of the Chinese Academy of Agricultural Sciences (Harbin, China), and maintained in Dulbecco's Modified Eagle's Medium (DMEM, Gibco, USA) supplemented with 10% fetal bovine serum (FBS, Gibco, USA), 100 U/mL of penicillin, and 100 μg/mL of streptomycin at 37 °C and 5% CO_2 (Wang et al., 2018). APP serotype 5 reference strain L20 (APP 5b L20) was obtained from the Shanghai Entry-Exit Inspection and Quarantine Bureau (Shanghai, China), and grown in brain-heart infusion broth (BHI, Difco Laboratories, Detroit, MI, USA) supplemented with 10 μg/mL of nicotinamide dinucleotide (NAD, Sigma-Aldrich, St. Louis, MO, USA) at 37 °C (Liu et al., 2017). PCV2 isolate CC1 (genotype 2b) (GenBank accession: JQ955679) was propagated in PCV2-free PK-15 cells. The TCID50 was measured by the Reed-Muench method.

2.2. Adherence and invasion assays

To compare the effect of prior, co-incident or post infection of PCV2 on the ability of APP to adhere or invade PAMs, 1×10^6 PAMs were infected with APP (MOI = 10:1) and/or PCV2 (MOI = 10:1) as outlined in Table 1. The control group for both the "PCV2-APP" and "PCV2 + APP" groups was the "APP2 h" group, a set of three duplicate wells for each group being used. To quantify the adherence of APP to PAMs, non-adherent bacteria were removed by washing five times with Dulbecco's Phosphate Buffered Saline (DPBS, Gibco, USA), followed by addition of 1 mL of 0.25% trypsin-EDTA (Gibco, USA) to release the bacteria that were adherent to the cells. The above liquid was diluted 1:1000, plated onto agar for 14 h, and the number of bacterial colonies counted. For the invasion assay, the cells were washed three times with DPBS buffer, and 1 mL of DMEM containing 100 μg/mL of gentamicin was added to each well, followed by incubation at 37 °C with 5% CO_2 for 1 h. Finally, PAMs were lysed with 1 mL of DMEM containing 1% (v/v) Triton X-100 (Sigma, USA) for 1 min after washing three times with DPBS buffer. PAM cell lysates (0.1 mL) were plated onto agar and incubated for 14 h and the number of bacterial colonies counted (Wang et al., 2015).

2.3. ROS level detection

A total of 1×10^6 PAMs were infected with APP (MOI = 10:1) or PCV2 (MOI = 10:1) or treated with 10 mM N-acetyl-L-cysteine (NAC, ROS scavenger, Beyotime, China) for 2, 4, and 6 h as follows: APP infection alone; PCV2 and APP coinfection; and APP infection with NAC pretreatment. The uninfected group served as the control, three duplicate wells for each treatment group were used. Then, the ROS-specific fluorescent probe 2′,7′-dichloroflurescin diacetate (DCFH-DA, Beyotime, China) was used to measure the total intracellular ROS levels. DCFH-DA (10μ mol/L) was added after infection, and the cells were incubated for 30 min at 37 °C and 5% CO_2. The results were visualized using a fluorescence microscope (Thermo, EVOS M5000), and the DCFH-DA fluorescence intensity was determined using ImageJ software (National Institutes of Health, USA). Intracellular bacteria were enumerated using the method described for the invasion assay (2.2).

2.4. MTT assay

A total of 5×10^4 PAMs were infected with APP (MOI = 10:1) and PCV2 (MOI = 10:1) for 2, 4, and 6 h as follows: APP infection alone; PCV2 infection alone; and PCV2 and APP coinfection. The uninfected group served as the control group, three duplicate wells for each treatment group were used. The MTT (3-(4,5-dimethylthiazol-2-yl)-2,5-diphenyl tetrazolium bromide) assay was used to assess PAM cytotoxicity. In brief, after infection, 20 μL of MTT (5 mg/mL) to each well was added, and cells incubated for 4 h at 37 °C. Subsequently, 150 μL of DMSO was added and, after a 10 min incubation, the optical density (OD) was measured at 490 nm using a microplate reader (BioTek, USA).

2.5. RT-qPCR

The infection method was the same as that described in Section 2.3. Total RNA was isolated from the PAMs using RNAiso Plus (TaKaRa, Japan) according to the manufacturer's protocol, and reverse-transcribed into cDNA using the Prime Script™ RT reagent kit (TaKaRa, Japan). A quantitative analysis of gene expression was performed using the TB Green™ Premix EX Taq™ (TaKaRa, Japan) and the Mxpro Mx3005 Real-Time QPCR System (Mxpro Mx3005, USA). The gene primers (Table 2) were synthesized by Comate Ltd. (Changchun, China). Relative gene expression was calculated using the Livak and Schmittgen $2^{-\Delta\Delta CT}$ method (Livak and Schmittgen, 2001) and normalized to goose β-actin.

2.6. Mitochondrial membrane potential detection

A total of 1×10^6 PAMs were infected with APP (MOI = 10:1) and PCV2 (MOI = 10:1) for 2, 4, and 6 h as follows: APP infection alone;

Table 1
The design of adherence and invasion assays.

No.	Name of group	Treatment description
1	PCV2-APP group	PAM was first infected with PCV2 for 2 hours, and then APP was added into the PAM-PCV2 mixture and co-cultured for 2 another hours.
2	PCV2 + APP group	PCV2 and APP simultaneously were added into PAM culture and co-cultured for 2 another hours.
3	APP-PCV2 group	APP and PAM were first co-cultured for 2 hours, and then PCV2 was added in and co-cultured for another 2 hours.
4	APP-2 h group	APP and PAM were co-cultured for 2 hours
5	APP-4 h group	APP and PAM were co-cultured for 4 hours

Table 2
Specific primers used for the RT-qPCR analysis in this study.

Gene	Forward primer (5' – 3')	Reverse primer (5' – 3')
β- actin	CATCACCATCGGCAACGA	GCGTAGAGGTCCTTCCTGA
IL-1β	CTAAGGAAAGCCATACCCAGAG	TTCAGGCAGCAACCATGTA
IL-6	CTCTGGAGCCCACCAAGAAC	TCCCAAGAAGGCAACTGGAT
TNF-α	CTACCTTGTTGCCTCCTCTTT	GAGCAGAGGTTCAGTGATGTAG
IFN-γ	AAATCCTGCAGAGCCAGATTAT	GCTGTTGCTGAAGAAGGTAGTA

PCV2 infection alone; and PCV2 and APP coinfection. The uninfected group served as the control group, three duplicate wells for each treatment group were used. The mitochondrial membrane potential was determined by fluorescence microscopy using a mitochondrial membrane potential assay kit with JC-1 (Beyotime, China) according to the manufacturer's instructions. The detection scheme was similar to that of the ROS test (2.3).

2.7. NADPH oxidase activity

The infection method was the same as that described in Section 2.6. The NADPH oxidase activity was measured with the Cellular NADPH Oxidase Activity Spectrophotometric Quantitative Detection Kit (Genmed Scientifics Inc., USA) according to the manufacturer's instructions. The absorbance value was measured at 340 nm on a microplate reader (TECAN). The optical density value is directly proportional to the NADPH oxidase activity.

2.8. In vivo experiments

Male (n = 36) and female (n = 36) ICR mice weighing 18–22 g were purchased from the Experimental Animal Center of Jilin University. All animal studies were conducted with the approval of the Institution Animal Care and Use Committee of Jilin University under approved protocol number JLUA-1309. This study was also approved by the Animal Center of Jilin University. The animals were allowed to adapt to the conditions for 2 days prior to experimentation.

(i) Infection experiments. Mice were infected with APP (6.5×10^7 CFU/20 μL) and PCV2 (1×10^8 copies/20 μL) intranasally under anaesthesia with 2.5% inhaled isoflurane. A total of 72 ICR mice were randomly divided into four groups as follows: control group (n = 9); PCV2 infection group (n = 9); APP infection group (n = 27); and PCV2 and APP coinfection group (n = 27). After infection for 6, 12 and 24 h, the clinical signs and body weights were recorded. The mice were sacrificed after anaesthesia, and samples were collected for further analysis.

(ii) Clinical signs. The mental status, activity status, appetite, eye secretions, and fur quality of mice were clinically scored. The scoring system was as follows: no clinical signs, 0; slight signs, 1; moderate signs, 2; and severe signs, 3 (Table 3).

(iii) Lung index. The lung weight of each mouse was recorded and compared to its body weight to obtain the lung index. Lung index = A/B, where A is the lung weight and B is the body weight.

(iv) Alveolar macrophage isolation and ROS detection. After the mice were sacrificed under anaesthesia, their thoraxes were dissected to expose the lungs. After the trachea was found in the neck of the mice, an indwelling needle was inserted and 1 mL phosphate-buffered saline (PBS, 0.2 mM EGTA and 0.2% bovine serum albumin) was slowly injected into the lungs. Lavagewas carried out three times. After red blood cell lysis, mouse alveolar macrophages were collected by centrifugation and resuspended in RPMI 1640 (Gibco) medium containing 10% FBS and seeded into 48-well plates for 30 min. Alveolar macrophages were washed with PBS to remove all non-adherent cells. The ROS detection method was the same as that described above (2.3).

(v) Determination of APP CFUs. To detect the numbers of APP in the lungs and alveolar macrophages at different time points, the lung homogenate and alveolar macrophage intracellular bacteria were appropriately diluted and cultured overnight on a BHI plate for colony counting.

(vi) ELISA assay. The cytokine IL-4, TNF-α and IFN-γ levels were measured using mouse-specific enzyme-linked immunosorbent assay (ELISA) kits (R&D, USA) according to the manufacturer's protocol.

2.9. Statistical analysis

Data are shown as the mean ± SD. The statistical analyses were performed using One-way ANOVA as implemented in SPSS version 19.0. $P < 0.05$ was considered statistically significant.

3. Results

3.1. PCV2 promoted APP adhesion to and invasion of PAMs

PAMs were infected with APP for 2 and 4 h as the control groups, preinfected with PCV2 for 2 h followed by infection with APP for 2 h as the PCV2-APP group, coinfected with PCV2 and APP for 2 h as the PCV2 + APP group, and preinfected with APP for 2 h followed by infection with PCV2 for 2 h as the APP-PCV2 group. The number of APP adhering to PAMs was greater in the APP-PCV2 group compared to that of the control group ($P < 0.01$) (Fig. 1A). The invasion of PAMs by APP was significantly higher in the PCV2-APP ($P = 0.047$), PCV2 + APP ($P = 0.031$), and APP-PCV2 ($P = 0.040$) compared to the control group. No significant difference was found between the PCV2-APP and PCV2 + APP groups ($P = 0.822$) (Fig. 1B). These results suggest that APP adhesion to and invasion of PAMs was increased by PCV2 infection.

3.2. PCV2 enhanced APP survival in PAMs by inhibiting ROS

ROS production was visualized by fluorescence microscopy (Fig. 2A). The results showed that the amount of ROS production in the coinfection group was less than in the APP infection group at 2 h ($P < 0.01$) (Fig. 2B), and that the number of intracellular bacteria were increased compared to that of the APP infection group ($P < 0.01$) (Fig. 2C). In the APP infection group, ROS production was increased after an additional 2 h. After 4 h of infection, ROS production was still lower in the coinfection group than that of the APP infection alone group ($P < 0.01$) (Fig. 2B), and the number of intracellular bacteria were still higher ($P < 0.01$) in the coinfection group compared to the APP infection group. However, the numbers of intracellular bacteria at 4 h were decreased compared to those at 2 h (Fig. 2C). After 6 h of infection, ROS production was decreased in both groups (Fig. 2B), and

Table 3
Clinical score.

Mental status		Activity status		Appetite		Fur		Eye secretion		Total score
normal	0	particularly active	0	normal	0	normal	0	no secretions, bright eyes	0	
glum	1	reduced active	1	occasionally to eat	1	less fur erect	1	less secretions	1	
depression	2	occasionally active	2	anorexia	2	moderate fur erect	2	more and purulent secretions	2	
coma	3	squats motionless	3	apastia	3	large area fur erect	3	solid secretions, eyes closed	3	

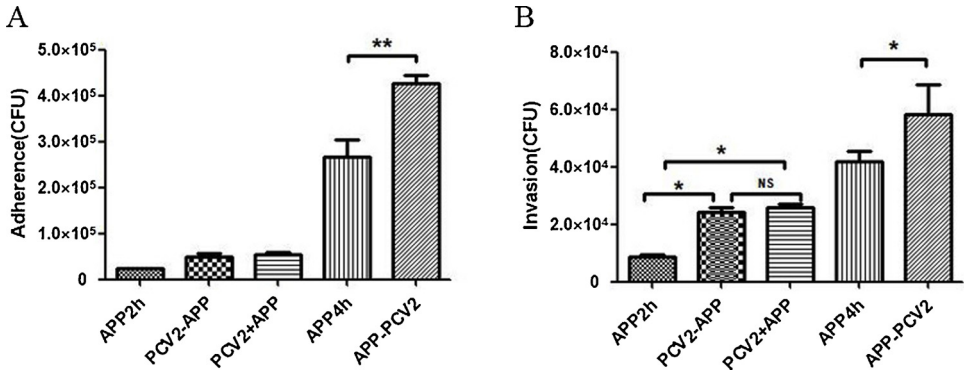

Fig. 1. APP adhesion to and invasion of PAMs was increased by PCV2 infection. (A). Adhesion assay. (B). Invasion assay. NS P > 0.05,*P < 0.05, **P < 0.01.

intracellular bacteria were almost eliminated (Fig. 2C).

ROS production was minimized when the PAMs were pretreated with the ROS scavenger NAC for 2 h and then infected with APP (P < 0.01) (Fig. 2B). The numbers of invading APP in the NAC treatment group were significantly higher at 2 and 4 h (P < 0.01), but were lower than in the PCV2 and APP coinfection groups (P < 0.01) (Fig. 2C).

The cytotoxicity of the PAMs was analysed by use of the MTT assay after pathogen infection. A lower OD value represents greater cytotoxicity. At both 2 and 4 h post-infection, the cytotoxicity of the APP infection and coinfection groups was significantly greater than that of the control group, and the cytotoxicity of the coinfection group was greater than that of the APP infection group (P < 0.01) (Fig. 2D). At 6 h post-infection, the cytotoxicity of the APP infection and coinfection groups reached their peak, but no difference was found between the two groups (P < 0.01) (Fig. 2D). These results indicated that PCV2 and APP coinfection resulted in the greatest cytotoxicity to PAMs.

3.3. PCV2 affected cytokine expression by PAMs during coinfection

The ability of PAMs to express cytokines was detected by quantitative real-time PCR. TNF-α and IFN-γ expression was greatest in the

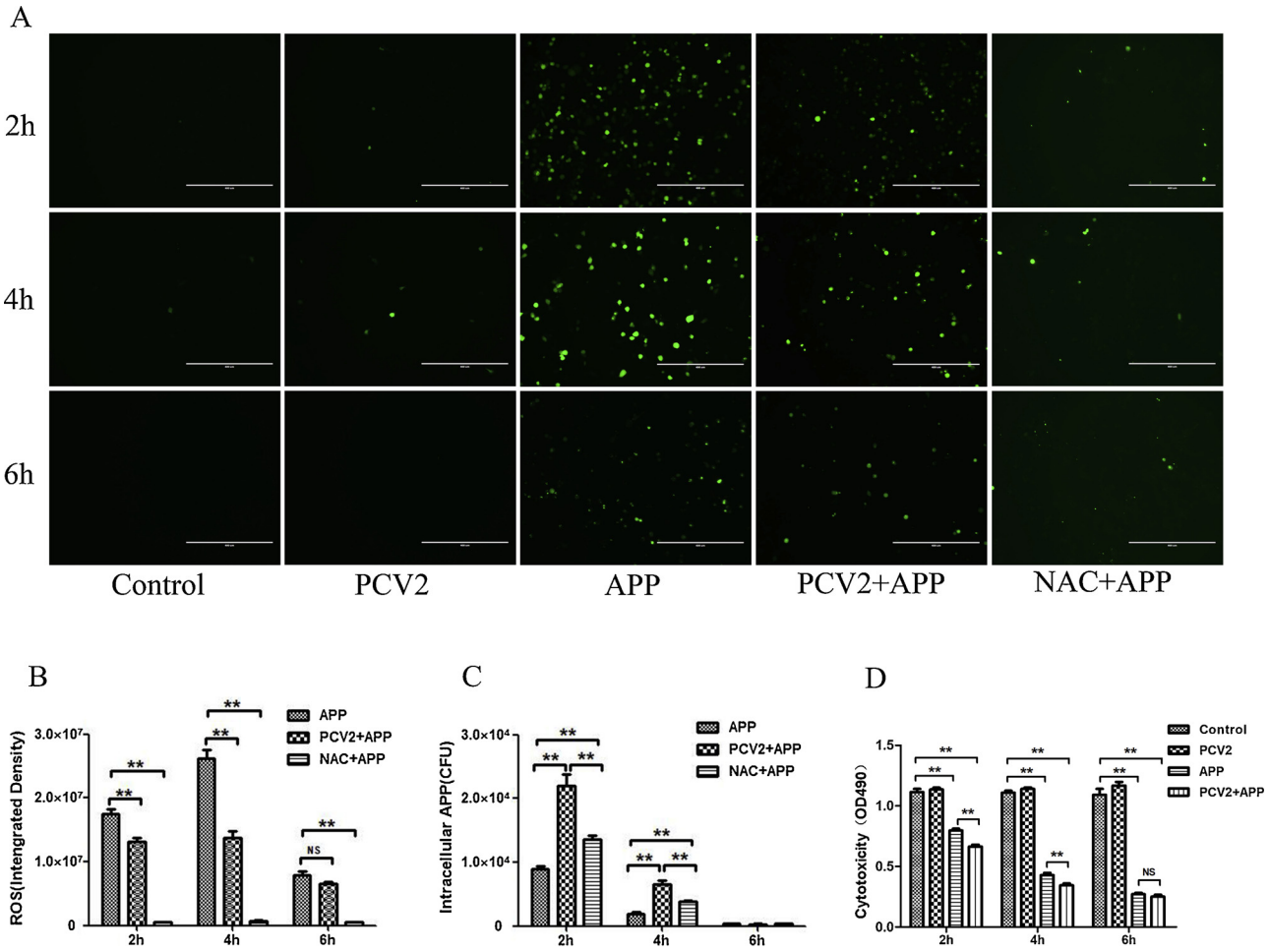

Fig. 2. PCV2 promoted intracellular survival of APP by inhibiting ROS production in the coinfection group. (A). ROS production was visualized by fluorescence microscopy. (B). The fluorescence intensity of DCFH-DA was determined using ImageJ software. (C). Intracellular APP detection. (D). Detection of cytotoxicity by MTT. NS P > 0.05,*P < 0.05, **P < 0.01.

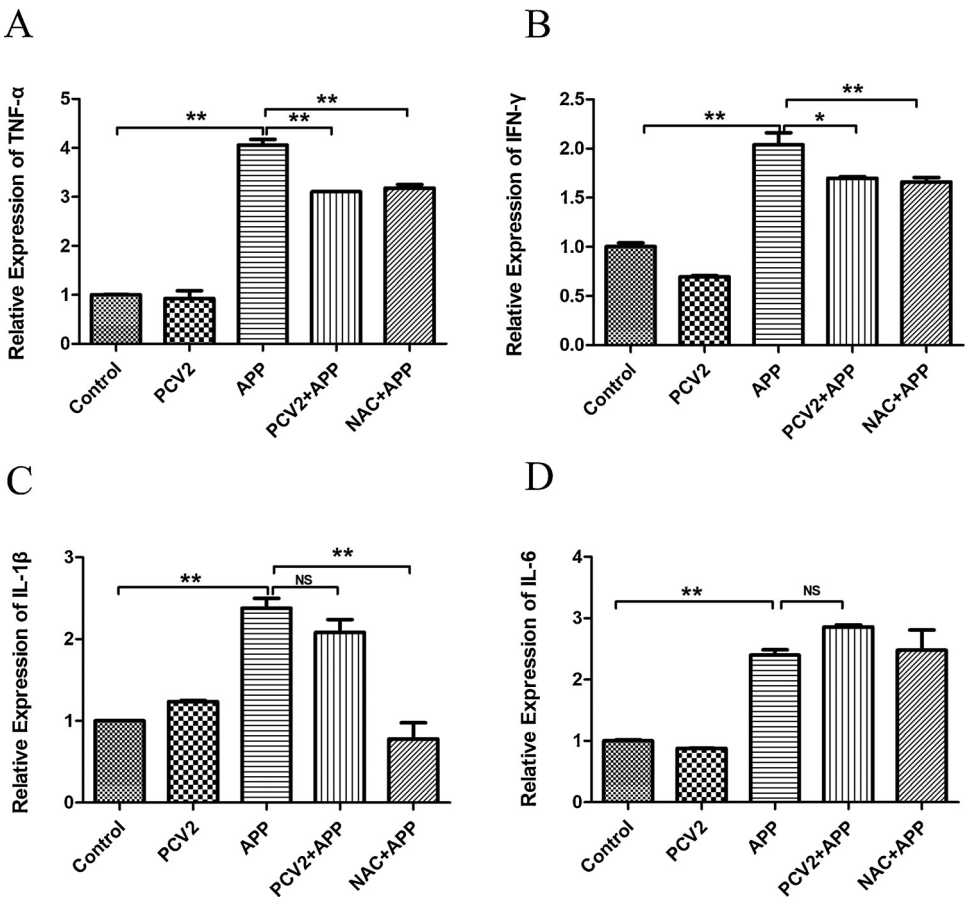

Fig. 3. PCV2 affected the expression of inflammation-associated cytokines. The ability of PAMs to secrete cytokines was detected by RT-qPCR. (A). TNF-α. (B). IFN-γ. (C). IL-1β. (D). IL-6. NS $P > 0.05$,*$P < 0.05$, **$P < 0.01$.

APP infection group ($P < 0.01$), although was significantly lower in the coinfection group compared to the APP infection group ($P < 0.05$) (Fig. 3A, B). IL-1β and IL-6 expression was higher in the APP infection group ($P < 0.01$), with no significant differences being found between the APP infection and coinfection groups (Fig. 3C, D). However, compared with the APP infection alone, the ability of PAMs to express TNF-α, IFN-γ, and IL-1β was significantly reduced when ROS was inhibited by NAC (an ROS scavenger) ($P < 0.01$). This reduction in proinflammatory cytokine expression may also be the result of ROS inhibition by PCV2.

3.4. PCV2 inhibited cell membrane NADPH oxidase activity during PCV2-APP coinfection

Next, we examined the sites of both ROS production after APP infection of PAMs, and PCV2-induced inhibition of ROS production during APP and PCV2 coinfection. The mitochondrial membrane potential was detected using fluorescent probe JC-1. Normal cells showed red fluorescence and green fluorescence when the mitochondrial membrane potential was altered (Fig. 4A). The results indicated that the proportion of PAMs with altered mitochondrial membrane potential was increased in both APP infection ($P < 0.01$) and coinfection groups ($P < 0.01$) compared to that of controls, whereas the mitochondrial membrane potential of the PCV2-infection group was unaltered ($P = 0.726$). No significant difference was observed in changes in the mitochondrial membrane potential between APP infection and coinfection groups ($P = 0.834$) (Fig. 4B). The mitochondrial membrane potential decreases due to depolarization when the mitochondria produce ROS. The results indicated that mitochondria produced and released ROS when infected with APP, whereas PCV2 did not affect mitochondrial ROS release.

The NADPH oxidase activity on the cell membrane reflects the ability of the cell to produce ROS. A cellular NADPH oxidase activity spectrophotometric quantitative detection kit was used to detect changes in NADPH oxidase activity in the PAMs. The results showed that PAMs infected with APP had significantly increased NADPH oxidase activity ($P < 0.01$) compared with that of the uninfected group, and that PCV2 infection was not associated with a change in NADPH oxidase activity. However, the NADPH oxidase activity in the coinfection group was significantly reduced compared to that in the APP infection group ($P = 0.023$) (Fig. 4C). These findings indicated that NADPH oxidase on the cell membrane could produce ROS after infection of PAMs with APP. Conversely, PCV2 inhibited the ability of the NADPH oxidase to produce ROS in the PCV2 and APP coinfection group.

3.5. In vivo validation of the ability of PCV2 to enhance APP survival

ICR mice were used to establish an APP and PCV2 coinfection model. The numbers of APP in the lungs and alveolar macrophages, and ROS production in alveolar macrophages were compared between the coinfection and APP infection groups. Simultaneously, we examined changes in the body weight, lung index, clinical signs, and lung lesions in each group of mice.

Six hours after infection was considered early infection. ROS production was lower in the coinfected group than in the APP-infected group ($P < 0.01$) (Fig. 5A, B). Compared to that in the APP-infected group, the numbers of intracellular bacteria in alveolar macrophages ($P = 0.019$) (Fig. 5C) and lung homogenates ($P < 0.01$) (Fig. 5D) were less than those in the coinfected group. The weight gains of mice in the

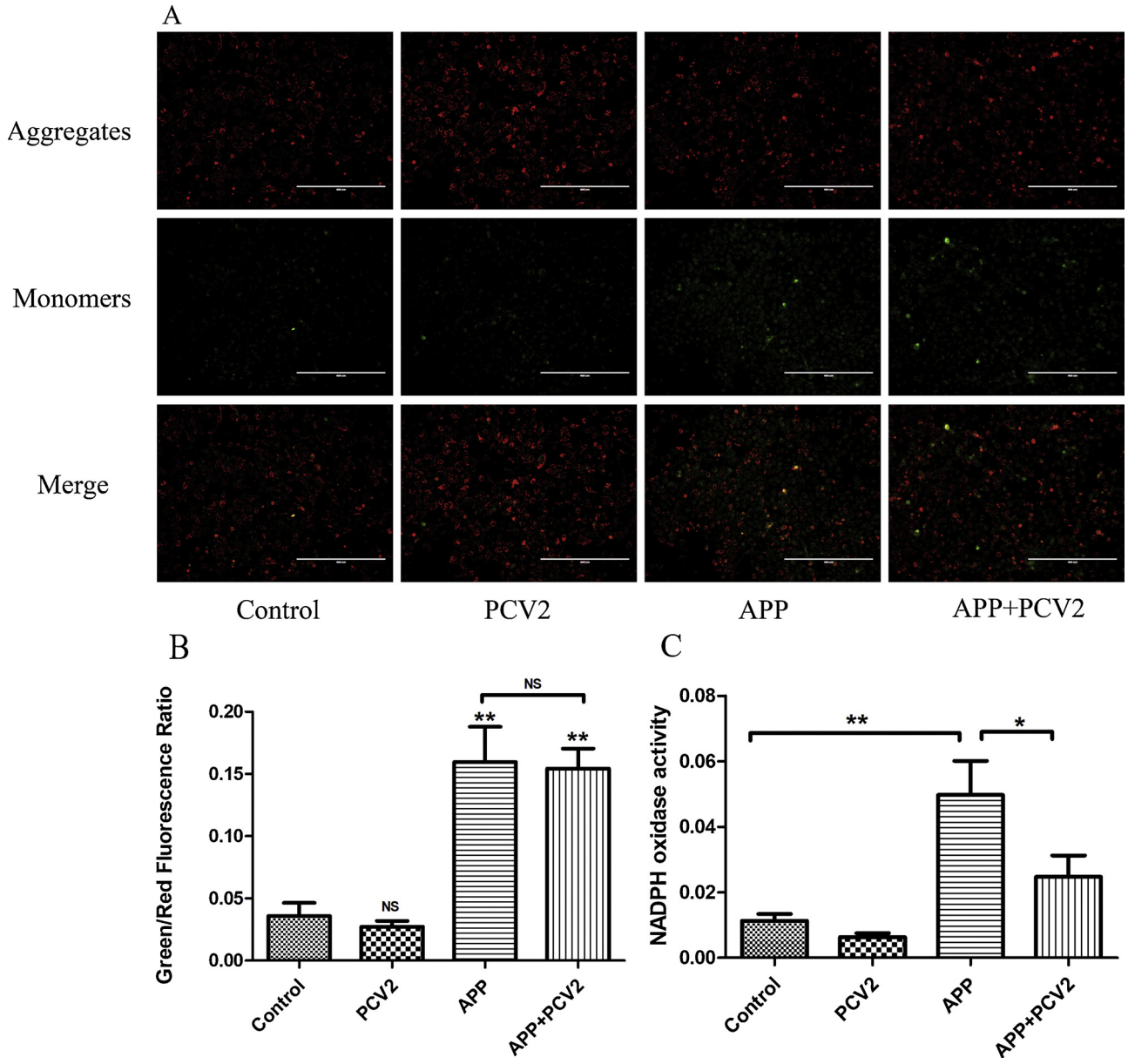

Fig. 4. Location of ROS production and inhibition after coinfection of PAMs with APP and PCV2. (A). Detection of PAM mitochondrial membrane potential by fluorescence microscopy. Mitochondrial aggregates did not produce ROS, whereas the mitochondrial monomers did produce ROS. (B).The fluorescence intensity of JC-1 was determined using ImageJ software. The green to red fluorescence ratio was calculated. (C). NADPH oxidase activity was detected by a spectrophotometric quantitative detection kit. The OD was measured at 340 nm on a microplate reader. NS $P > 0.05$,*$P < 0.05$, **$P < 0.01$. (For interpretation of the references to colour in this figure legend, the reader is referred to the web version of this article).

control, PCV2 infection, APP infection, and coinfection groups were 0.74 ± 0.14 g, 0.30 ± 0.33 g, 0.04 ± 0.13 g, and -0.14 ± 0.11 g, respectively (Fig. 5E). The mouse weights were lower in the APP infection ($P = 0.031$) and coinfection ($P < 0.01$) groups than in the control group. The lung indexes of the mice in the four groups were 0.0099 ± 0.0007, 0.0100 ± 0.0010, 0.0125 ± 0.0019, and 0.0143 ± 0.0053, respectively (Fig. 5F). The lung index of the coinfection group was significantly higher than that of the APP infection group. All mice in the infected groups showed signs of a poor mental state, loss of appetite, and gathered together in the corner of cages. (Fig. 5G). The pathological changes of slight hemorrhage and edema were observed in both the APP infection and coinfection groups (Fig. 5H).

Twelve hours after infection was considered mid-term infection. ROS production increased in the coinfection group to a level significantly higher than that in the APP infection group ($P < 0.01$) (Fig. 5A, B). As a result, the number of bacteria were reduced in both lung homogenates ($P < 0.01$) (Fig. 5D) and alveolar macrophages ($P < 0.01$) (Fig. 5C). The weight gains of the mice in the four groups listed above were 0.95 ± 0.13 g, 0.59 ± 0.46 g, −0.26 ± 0.27 g, and −0.51 ± 0.25 g, respectively (Fig. 5E). The mice lost weight severely in the APP infection ($P < 0.01$) and coinfection groups ($P < 0.01$). The lung indexes of the mice in the four groups were 0.0077 ± 0.0004, 0.0072 ± 0.0010, 0.0191 ± 0.0067, and 0.0254 ± 0.0012, respectively (Fig. 5F). The lung index of mice increased significantly in the APP infection group ($P < 0.01$), and was significantly higher in the coinfection group compared to the APP infection group ($P < 0.01$). The clinical signs of the mice were alleviated in the PCV2 infection group. The mice exhibited loss of appetite, closed eyes and loss of movement in the APP infection and coinfection groups (Fig. 5G). Severe pulmonary edema occurred in the APP infection and coinfection groups, and severe bleeding was found in the coinfection group

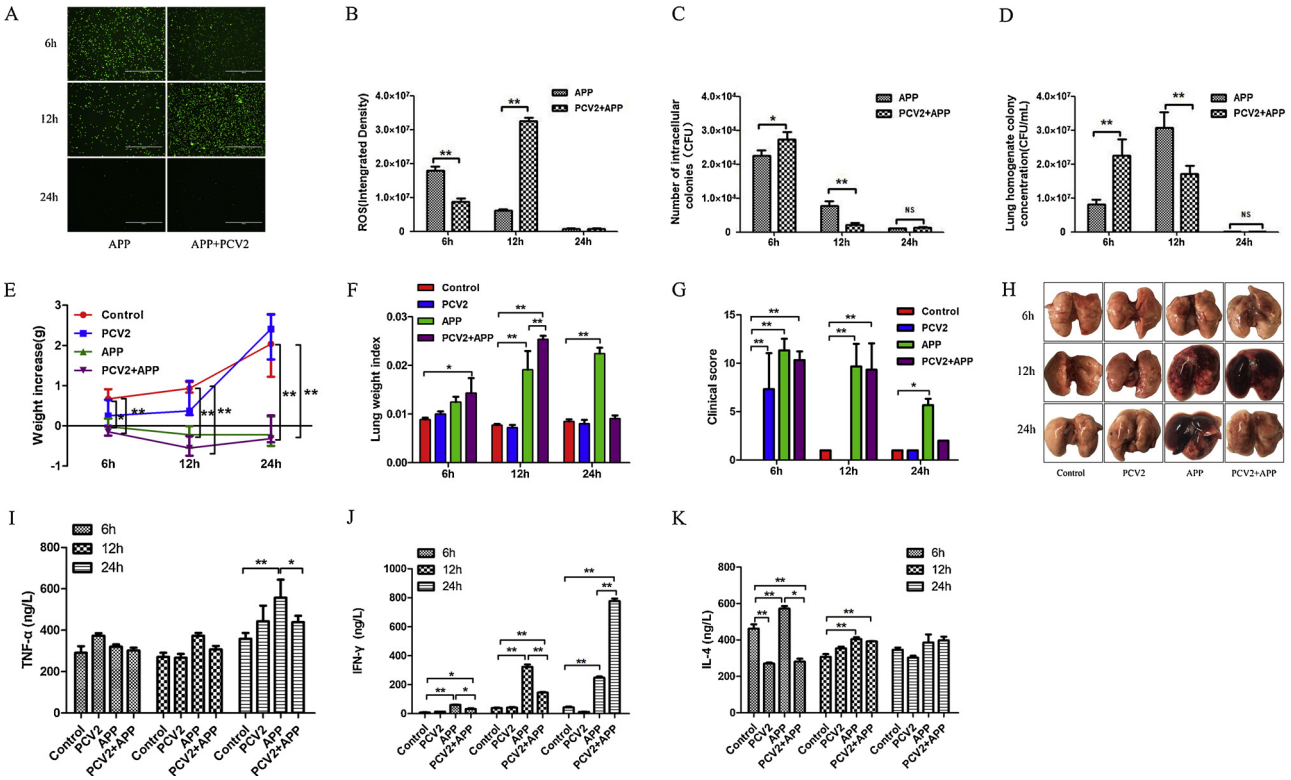

Fig. 5. Coinfection in animals. (A). ROS production was visualized by fluorescence microscopy. (B).The fluorescence intensity of DCFH-DA was determined using ImageJ software. (C). Bacterial loads in mouse alveolar macrophages. (D) Bacterial loads in the mouse lung. (E). Weight gain after infection. (F). Lung index = the lung weight / the body weight. (G). Recorded clinical scores at each time point after infection. (H). Macroscopic changes of the lung. (I). The TNF-α expression level. (J). The IFN-γ expression level. (K). The IL-4 expression level. NS $P > 0.05$,*$P < 0.05$, **$P < 0.01$.

(Fig. 5H).

Twenty-four hours after infection was considered late infection. The ROS levels were lowest in the coinfection and APP infection groups. The numbers of bacteria in the lung and alveolar macrophages were minimized, and no significant difference was found between the two groups (Fig. 5A–D). The weight gains of the mice in the four groups listed above were 2.01 ± 0.78 g, 2.28 ± 0.58 g, -0.16 ± 0.37 g, and -0.16 ± 0.36 g, respectively (Fig. 5E). The mice lost weight severely in the APP infection ($P < 0.01$) and coinfection groups ($P < 0.01$). The lung indexes of the mice in the four groups were 0.0085 ± 0.0007, 0.0080 ± 0.0014, 0.0224 ± 0.0021, and 0.0091 ± 0.0011, respectively (Fig. 5F). Compared to those of the other groups, the lung index of the mice was increased significantly in the APP infection group ($P < 0.01$). The clinical signs of the mice were still serious in the APP infection group (Fig. 5G), and the lungs showed extensive bleeding (Fig. 5H). The clinical signs and lung lesions of the mice were alleviated in the coinfection group.

TNF-α, IFN-γ and IL-4 expression levels in lung homogenates were detected by ELISA. At 24 h post-infection, TNF-α release was significantly increased in the APP infection group ($P < 0.01$) but was lower in the coinfection group than in the APP infection group ($P = 0.04$) (Fig. 5I). At both 6 and 12 h post-infection, IFN-γ secretion was significantly higher in the APP infection ($P < 0.01$) and coinfection ($P < 0.05$) groups, but was lower in the coinfection group than in the APP infection group ($P < 0.05$). At 24 h post-infection, IFN-γ secretion was significantly higher in APP infection ($P < 0.01$) and coinfection ($P < 0.01$) groups, but was significantly higher in the coinfection group compared to that in the APP infection group ($P < 0.01$) (Fig. 5J). At 6 h post-infection, IL-4 secretion was significantly lower in the PCV2 infection and coinfection groups than in the control and APP infection groups ($P < 0.05$). At 12 h post-infection, IL-4 secretion was significantly higher in the APP infection and coinfection groups than in the control group ($P < 0.01$), and no significant difference was found between the two groups (Fig. 5K). Similar to the in vitro cell experiments, TNF-α and IL-4 secretion in the lung was reduced by PCV2 during coinfection. IFN-γ release was also reduced by PCV2 during coinfection at the early stage. However, IFN-γ secretion was higher at the later stage during coinfection, which might be related to viral proliferation.

4. Discussion

In this study, we found that PCV2 promoted APP adhesion to, invasion of, and survival in alveolar macrophages during PCV2 and APP coinfection in vitro and in vivo. Additionally, we found that PCV2 effectively inhibited ROS production in macrophages, thereby reducing the bactericidal capacity of ROS and contributing to APP survival. At the same time, an increased number of bacteria was associated with greater macrophage cytotoxicity. These two important pathogens are components of the PRDC; indeed, coinfection of PCV2 with other bacteria is frequently diagnosed (Kim et al., 2003), and pigs infected with APP have a high mortality rate (Sassu et al., 2018). Better understanding of viral-bacterial coinfection mechanisms will provide an opportunity to develop new therapeutic approaches and preventative strategies. During the early period, the use of antiviral drugs and vaccines could reduce secondary bacterial infections associated with primary viral infection. These findings provide a valuable reference for greater understanding of the PRDC, a substantial problem in intensive pig farms worldwide.

Previous studies have provided many examples of a virus promoting a bacterial coinfection. The macrophage apoptotic response against *Mycobacterium tuberculosis*, mediated by TNF-α, was shown to be impaired by human immunodeficiency virus promoting bacterial survival (Patel et al., 2007). Influenza virus enhanced the intestinal colonization

and systemic transmission of *Salmonella* through Type I interferons (Deriu et al., 2016). However, the harm caused by PCV2 and APP co-infection has not been studied to date, and this study fills this gap. PCV2 or APP can damage alveolar macrophages when they invade the lungs (Chang et al., 2006a; Wang et al., 2015). Many reports have studied ROS in individual microbial infections. For instance, *Vibrio parahaemolyticus* utilizes its T3SS2 effector VopL to promote intracellular survival by inhibiting the host ROS response (Santos et al., 2017). However, few studies have evaluated the important role of ROS in co-infections of various microorganisms. In this study, we found that PCV2 effectively inhibited NADPH oxidase activity on the macrophage membrane, which reduced ROS production. This process could facilitate APP survival in PAMs. The proinflammatory cytokines IL-1β and IL-6 were highly expressed by PAMs during APP infection and coinfection. However, TNF-α, and IFN-γ showed downregulation during coinfection, which suggests that PCV2 can weaken the inflammatory response by reducing the expression of inflammatory cytokines during coinfection, thereby promoting the intracellular survival of APP.

Regarding adherence to PAMs, we found the similar values for both the APP-2 h and PCV2 + APP groups. A possibility is that there is a powerful phagocytic function of PAMs when infected for 2 h, with PAMs engulfing most of the APP adhered to the cell surface. However, the number of APP adherent to PAMs increased with the involvement of PCV2 at 4 h after infection. We speculate that prior PCV2 infection inhibits ROS production by PAMs and this leads to reduced clearance of engulfed APP. More APP living in cells would constantly destroy PAMs, which may affect their phagocytic function. At the early stage of infection, PCV2 promoted APP intracellular survival by inhibiting ROS production by PAMs, but more APP were present in the PCV2 + APP group than the NAC + APP group. We speculate that PCV2 promoted APP survival in PAMs by not only inhibiting ROS but also via other mechanisms, such as inhibition of antigen presentation (Yang et al., 2017), Type I interferon (IFN) expression (Choi et al., 2018), and/or cellular signaling pathways (Wei et al., 2009). We used ICR mice as a model to study APP and PCV2 coinfection and evaluated clinical sign indexes and the relationship between ROS production and APP invasion in the lungs. At 6 h after infection, the mice lost weight and pneumonedema accompanied by severe clinical signs occurred in both the APP infection and coinfection groups. Similar ROS levels and APP counts were found in vitro and in vivo. These phenomena further confirmed that PCV2 promoted APP invasion into the lung and alveolar macrophages by inhibiting ROS release during the early stages of coinfection. At 12 h after infection, the mice had severe weight loss, lung hemorrhage and edema in the APP infection and coinfection groups. The degree of lung lesions was more severe in the coinfection group than in the APP infection group. Interestingly, compared to that in the APP infection group, ROS production was significantly higher in the coinfection group. These phenomena should be PCV2 no longer to inhibit ROS production, which also causes oxidative stress in alveolar macrophages. Excessive ROS is able to aggravate tissue damage, disrupt cell metabolism, and induce apoptosis (Vannella and Wynn, 2017). At 24 h after infection, the mice reached the convalescence phase. During this period, the amount of bacteria and ROS were both at their lowest in alveolar macrophages compared to the other stages. Pulmonary lesions and clinical signs were alleviated in the coinfection group but remained highly apparent in the APP infection group. We hypothesized that PCV2 initiated some protective mechanisms in the lungs to enable continuous proliferation in this organ. ELISA was used to detect cytokine expression levels in the lung, including TNF-α and IFN-γ (which promote the inflammatory response) and IL-4 (which promotes macrophage antigen presentation). Consistent with the in vitro cellular experimental results, PCV2 was associated with reduced cytokine expression during coinfection. This phenomenon is beneficial because it affects the inflammatory response and the antigen presentation function of macrophages and thus promotes APP survival.

5. Conclusion

In this study, we discovered that PCV2 promotes APP adhesion, invasion and survival in PAMs during coinfection. PCV2 decreased ROS production to contribute to APP survival in alveolar macrophages by inhibiting cytomembrane NADPH oxidase activity. PCV2 also weakened the inflammatory response and promoted APP survival by decreasing the expression of inflammation-related cytokines. The survival of higher numbers of APP causes stronger cytotoxicity for the cells. In vitro cellular experimental results were verified in vivo. Our findings may provide a deeper understanding of porcine coinfection, and will be extremely helpful for the design of strategies for PRDC control.

Compliance with ethical standards

All animal experiments complied with the specified regulations under the “Laboratory animal-Guideline for ethical review of animal welfare (GB/T 35892-2018)”. The protocols were reviewed by the Institutional Animal Care and the Committee of Jilin University and approved under protocol number JLUA-1309. The specific housing conditions for mice were as follows: the temperature of breeding environment 24 ℃, daily temperature difference ≤ 3℃, relative humidity up to 40%˜70%, fresh air ventilation l0 times/hour, air velocity ≤ 0.18 m/s, atmospheric pressure difference 25 Pa, cleanliness level ten thousand, ammonia concentration l5 mg/m^3, noise ≤ 60 dB, and intensity of illumination up to 150˜300 lx.

Conflict of interest

The authors declare no financial or commercial conflicts of interest.

Acknowledgments

This study was supported by the “National Natural Science Foundation of China” (No. 31520103917).

References

Allard, B., Panariti, A., Martin, J.G., 2018. Alveolar macrophages in there solution of inflammation, tissue repair, and tolerance to infection. Front. Immunol. 9, 1777.
Banoth, B., Cassel, S., 2018. Mitochondria in innate immune signaling. Transl. Res. 202, 52–68.
Bossé, J.T., Janson, H., Sheehan, B.J., Beddek, A.J., Rycroft, A.N., Kroll, J.S., Langford, P.R., 2002. *Actinobacillus pleuropneumoniae*: pathobiology and pathogenesis of infection. Microbes Infect. 4, 225–235.
Byrne, A.J., Mathie, S.A., Gregory, L.G., Lloyd, C.M., 2015. Pulmonary macrophages: key players in the innate defence of the airways. Thorax. 70, 1189–1196.
Chang, H.W., Jeng, C.R., Lin, T.L., Liu, J.J., Chiou, M.T., Tsai, Y.C., Chia, M.Y., Jan, T.R., Pang, V.F., 2006a. Immunopathological effects of porcine circovirus type 2 (PCV2) on swine alveolar macrophages by in vitro inoculation. Vet. Immunol. Immunopathol. 110, 207–219.
Chang, H.W., Pang, V.F., Chen, L.J., Chia, M.Y., Tsai, Y.C., Jeng, C.R., 2006b. Bacterial lipopolysaccharide induces porcine circovirus type 2 replication in swine alveolar macrophages. Vet. Microbiol. 115, 311–319.
Cheong, Y., Oh, C., Lee, K., Cho, K.H., 2017. Survey of porcine respiratory disease complex-associated pathogens among commercial pig farms in Korea via oral fluid method. J. Vet. Sci. 18, 283–289.
Chiers, K., De Waele, T., Pasmans, F., Ducatelle, R., Haesebrouck, F., 2010. Virulence factors of *Actinobacillus pleuropneumoniae* involved in colonization, persistence and induction of lesions in its porcine host. Vet. Res. 41, 65.
Choi, C.Y., Choi, Y.C., Park, I.B., Lee, C.H., Kang, S.J., Chun, T., 2018. ORF5 protein of porcine circovirus type 2 enhances viral replication by dampening type I interferon expression in porcine epithelial cells. Vet. Microbiol. 226, 50–58.
Deriu, E., Boxx, G.M., He, X., Pan, C., Benavidez, S.D., Cen, L., Rozengurt, N., Shi, W., Cheng, G., 2016. Influenza virus affects intestinal microbiota and secondary *Salmonella* infection in the gut through Type I interferons. PLoS Pathog. 12, e1005572.
Dione, M., Masembe, C., Akol, J., Amia, W., Kungu, J., Lee, H., Wieland, B., 2018. The importance of on-farm biosecurity: sero-prevalence and risk factors of bacterial and viral pathogens in smallholder pig systems in Uganda. Acta Trop. 187, 214–221.
Ge, X., Wang, F., Guo, X., Yang, H., 2012. Porcine circovirus type 2 and its associated diseases in China. Virus Res. 164, 100–106.
Haimi-Hakala, M., Hälli, O., Laurila, T., Raunio-Saarnisto, M., Nokireki, T., Laine, T., Nykäsenoja, S., Pelkola, K., Segales, J., Sibila, M., Oliviero, C., Peltoniemi, O.,

Pelkonen, S., Heinonen, M., 2017. Etiology of acute respiratory disease in fattening pigs in Finland. Porcine Health Manag. 3, 19.
Joshi, N., Walter, J.M., Misharin, A.V., 2018. Alveolar macrophages. Cell. Immunol. 330, 86–90.
Kim, J., Chung, H.K., Chae, C., 2003. Association of porcine circovirus 2 with porcine respiratory disease complex. Vet. J. 166, 251–256.
Lam, G.Y., Huang, J., Brumell, J., 2012. The many roles of NOX2 NADPH oxidase-derived ROS in immunity. Semin. Immunopathol. 32, 415–430.
Liu, J., Ma, Q., Yang, F., Zhu, R., Gu, J., Sun, C., Feng, X., Du, C., Langford, P.R., Han, W., Yang, J., Lei, L., 2017. B cell cross-epitope of *Propionibacterium acnes* and *Actinobacillus pleuropneumoniae* selected by phage display library can efficiently protect from *Actinobacillus pleuropneumoniae* infection. Vet. Microbiol. 205, 14–21.
Livak, K., Schmittgen, T., 2001. Analysis of relative gene expression data using real-time quantitative PCR and the 2(-Delta Delta C(T)) Method. Methods 25, 402–408.
McCallum, K., Garsin, D., 2016. The role of reactive oxygen species in modulating the *Caenorhabditis elegans* immune response. PLoS Pathog. 12, e1005923.
Meng, X.J., 2013. Porcine circovirus type 2 (PCV2): pathogenesis and interaction with the immune system. Annu. Rev. Anim. Biosci. 1, 43–64.
Murray, P.J., Wynn, T.A., 2011. Protective and pathogenic functions of macrophage subsets. Nat. Rev. Immunol. 11, 723–737.
Opriessnig, T., Giménez-Lirola, L.G., Halbur, P.G., 2011. Polymicrobial respiratory disease in pigs. Anim. Health Res. Rev. 12, 133–148.
Patel, N.R., Zhu, J., Tachado, S.D., Zhang, J., Wan, Z., Saukkonen, J., Koziel, H., 2007. HIV impairs TNF-alpha mediated macrophage apoptotic response to *Mycobacterium tuberculosis*. J. Immunol. 179, 6973–6980.
Pomorska-Mól, M., Dors, A., Kwit, K., Kowalczyk, A., Stasiak, E., Pejsak, Z., 2017. Kinetics of single and dual infection of pigs with swine influenza virus and *Actinobacillus pleuropneumoniae*. Vet. Microbiol. 201, 113–120.
Santos, M., Salomon, D., Orth, K., 2017. T3SS effector VopL inhibits the host ROS response, promoting the intracellular survival of *Vibrio parahaemolyticus*. PLoS Pathog. 13, e1006438.
Sassu, E.L., Bossé, J.T., Tobias, T.J., Gottschalk, M., Langford, P.R., Hennig-Pauka, I., 2018. Update on *Actinobacillus pleuropneumoniae*-knowledge, gaps and challenges. Transbound. Emerg. Dis. 65, 72–90.
Scialò, F., Fernández-Ayala, D., Sanz, A., 2017. Role of mitochondrial reverse electron transport in ROS signaling: potential roles in health and disease. Front. Physiol. 8, 428.
Thanawongnuwech, R., Brown, G.B., Halbur, P.G., Roth, J.A., Royer, R.L., Thacker, B.J., 2000. Pathogenesis of porcine reproductive and respiratory syndrome virus-induced increase in susceptibility to *Streptococcus suis* infection. Vet. Pathol. 37, 143–152.
Vannella, K.M., Wynn, T.A., 2017. Mechanisms of organ injury and repair by macrophages. Annu. Rev. Physiol. 79, 593–617.
Vlahos, R., Selemidis, S., 2014. NADPH oxidases as novel pharmacologic targets against influenza A virus infection. Mol. Pharmacol. 86, 747–759.
Wang, L., Qin, W., Ruidong, Z., Liu, S., Zhang, H., Sun, C., Feng, X., Gu, J., Du, C., Han, W., Langford, P.R., Lei, L., 2015. Differential gene expression profiling of *Actinobacillus pleuropneumoniae* during induction of primary alveolar macrophage apoptosis in piglets. Microb. Pathog. 78, 74–86.
Wang, T.Y., Liu, Y.G., Li, L., Wang, G., Wang, H.M., Zhang, H.L., Zhao, S.F., Gao, J.C., An, T.Q., Tian, Z.J., Tang, Y.D., Cai, X.H., 2018. Porcine alveolar macrophage CD163 abundance is a pivotal switch for porcine reproductive and respiratory syndrome virus infection. Oncotarget. 9, 12174–12185.
Wei, L., Zhu, Z., Wang, J., Liu, J., Wei, L., 2009. JNK and p38 Mitogen-activated protein kinase pathways contribute to porcine circovirus Type 2 infection. J. Virol. 83, 6039–6047.
Yang, N., Qiao, J., Liu, S., Zou, Z., Zhu, L., Liu, X., Zhou, S., Li, H., 2017. Change in the immune function of porcine iliac artery endothelial cells infected with porcine circovirus type 2 and its inhibition on monocyte derived dendritic cells maturation. PLoS One 12, e0186775.